

Preliminary Study of Using Colloidal $\text{SiO}_2@\text{ZrO}_2$ Particles in Recovering Actinides from Water and Immobilizing them in a Glass-Ceramic

Pablo M. Arnal^{1,2,}, Ariana Salvia²*

¹ Faculty of Exact Sciences, National University of La Plata, 47 y 115, 1900, La Plata, Province of Buenos Aires, Republic of Argentina.

² Ceramic and Mineral Resources Technology Center, National Scientific and Technical Research Council, National University of La Plata & Scientific research commission of the province of Buenos Aires, Camino Centenario y 506, CC 49, B1897ZCA, M. B. Gonnet – La Plata, Province of Buenos Aires, Republic of Argentina.

Corresponding author:

* E-mail: arnal@quimica.unlp.edu.ar

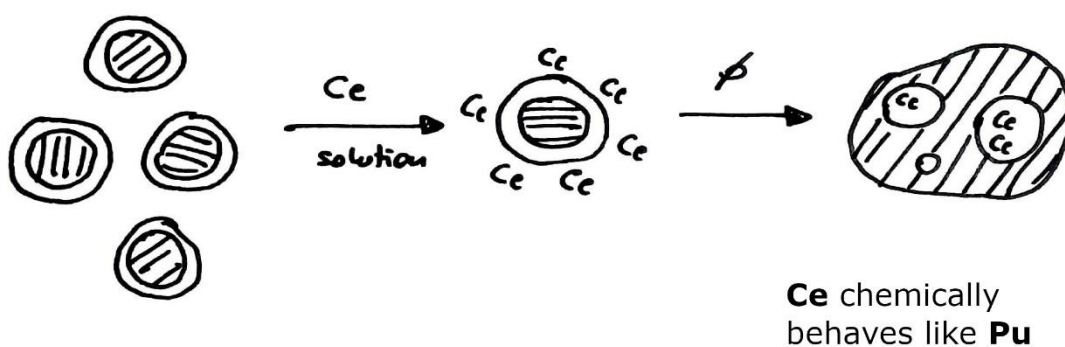
Abstract

Actinides, which are toxic for humans, increased their presence in the hydrosphere over the last 80 years. Though actinide recovery from water and immobilization for safe storage is technically feasible, it remains a complex process. Herein, we preliminary studied $\text{SiO}_2@\text{ZrO}_2$ in recovering actinides from water and trapping them in a glass-ceramic upon thermal treatment. To simplify our experimental work, we surrogated radioactive actinides with stable cerium. In the first part of the work, we tested $\text{SiO}_2@\text{ZrO}_2$'s ability to recover Ce from water in batch systems. Then, we thermally treated $\text{SiO}_2@\text{ZrO}_2$ with Ce to form a glass-

ceramic. All batch experiments showed that $\text{SiO}_2@\text{ZrO}_2$ removes Ce from water. Moreover, all experiments show that $\text{SiO}_2@\text{ZrO}_2$ with Ce converts into a glass-ceramic upon thermal treatment. When heated up to 1000 °C, particles remained spherical, and Ce remained trapped within the structure of crystalline spheroids located between the outer surface and a 50 nm depth. When heated up to 1450 °C, sintering produced bigger particles than the original colloid, and Ce remained trapped within the structure of crystalline spheroids having a broad size distribution located everywhere in the particles.

Keywords: plutonium surrogate; cerium; silicon oxide; zirconium oxide; core@shell; glass-ceramic; nuclear fuel cycle; environmental remediation; water decontamination;

Graphical abstract



1. Introduction

Actinides may endanger human life when waterborne. This danger results because actinides, which include a few naturally occurring elements and other artificial ones, are radioactive. Radioactivity produces new isotopes and releases high-energetic radiation. That energy is toxic to human beings.

The use of actinides in modern life had the unfortunate consequence of releasing radioactive elements into the geosphere [1]. Radioactive isotopes may originate in everyday devices such as smoke detectors. However, the primary source of actinides is nuclear weapons and fuels. Once intentionally or accidentally released[1], actinides may be transported worldwide by the hydrosphere [1], [2].

Well-established processes may recover waterborne actinides. For example, solvent extraction, precipitation/coprecipitation, and ion exchange procedures—all of them have been playing a pivotal role in the discovery and characterization of the 5f transition elements [3], [4][4]—are viable processes.

Once recovered, some actinides must be stored safely for long periods. This long storage—some actinides have long half-lives—may be performed by trapping actinides either in a glass or a glass-ceramic. These host materials should retain the radioactive isotopes that form during the radioactive decay and should resist the high energy radiation emitted during radioactivity [5]. Among the different materials for storing Pu, some glass-ceramic stands out [5] because of their ability to trap Pu within the crystalline zirconium oxide spheroids embedded in a silica matrix [6].

Over many decades, much knowledge about the recovery and immobilization of actinides surged. However, solid-solution separation and in situ immobilization techniques need further development [4] and are an attractive research field. So far, the research focus has been mainly placed either on recovery or immobilization of actinides. Although the

sequential application of those processes may allow recovery and immobilization, these processes are both costly and time-consuming [7]. Hence, new ways to recover and immobilize actinides are welcome.

The goal of this study was to preliminary investigate the potential of $\text{SiO}_2@\text{ZrO}_2$ —colloidal, monodisperse spheres with a silica core and zirconium oxide nanometer-thick and nanostructured shell [8][9]— in (a) recovering Pu from water and (b) trapping Pu within a glass-ceramic. Previous studies have shown $\text{SiO}_2@\text{ZrO}_2$'s ability to remove some actinides, including Pu from acid solutions [10] and $\text{SiO}_2@\text{ZrO}_2$'s potentiality to form glass-ceramics [8]. However, because Pu's radioactivity requires working under extraordinary safe conditions, we opted in this study for simplifying our experimental approach by surrogating Pu with Ce (a non-radioactive surrogate of Pu already used in many chemical studies [11]–[16]).

The hypotheses of this study were (a) that Ce in aqueous solution binds to $\text{SiO}_2@\text{ZrO}_2$ in batch systems, and (b) that $\text{SiO}_2@\text{ZrO}_2$ with cerium bound to its surface ($\text{SiO}_2@\text{ZrO}_2\text{-Ce}$) transforms upon thermal treatment into a glass-ceramic that traps cerium atoms within spheroidal crystals of ZrO_2 embedded in a silica matrix.

2. Materials and Methods

Chemicals. TEOS 98%. Ethanol 96%. Ammoniac solution 30%. Zirconium butoxide 80%. Distilled water. $(\text{NH}_4)_2\text{Ce}(\text{SO}_4)_4 \cdot 2\text{H}_2\text{O}$. Sulfuric acid. Lutensol AO5.

Synthesis of Colloidal $\text{SiO}_2@\text{ZrO}_2$. The synthesis of colloidal spherical $\text{SiO}_2@\text{ZrO}_2$ particles has been described previously [9]. A mixture of absolute ethanol (64 g) and an aqueous solution of NH_3 (22 g) in a closed 500 mL one-neck flask in a water bath (33 °C) was heated under stirring. A few minutes after injecting TEOS (4.2 mL) through the septum, the transparent solution turned into white stable dispersion of monodisperse silica spheres. After 60 min, the liquid phase of the colloid was exchanged for ethanol by centrifuging (5000 rpm, 5 min) and redispersing in ethanol (100 g) three times. The monodisperse silica spheres dispersed in absolute ethanol (100 g) were poured in a 500 mL one-neck flask, the flask was closed with a septum, and the dispersion was heated under stirring in a water bath (33 °C). After 30 min, 0.5 mL of an amphiphilic surfactant (0.43 g Lutensol AO5 in 11 g H_2O) were injected. After an additional 60 min, 1.8 mL of zirconium butoxide was injected. The reaction was allowed to continue overnight. The next day, the liquid phase of the colloid was exchanged for H_2O by centrifuging (5000 rpm, 5 min) and redispersing in H_2O (100 g) four times. The colloidal dispersion of monodisperse silica spheres in water was aged in a closed polypropylene flask (30 °C, three days). The solid (monodisperse $\text{SiO}_2@\text{ZrO}_2$ particles) was recovered by centrifuging (5000 rpm, 5 min) and dried (150 °C, 1 day).

The synthesis was performed two times. Both solid products were mixed before characterizing and further using.

Cerium Acid Aqueous Solutions. Two cerium solutions, **C1** and **C2**, were prepared. Both powdered $(\text{NH}_4)_2\text{Ce}(\text{SO}_4)_4 \cdot 2\text{H}_2\text{O}$ (0.9044 g) and aqueous sulfuric acid (1 M) were added to a 10.00 mL volumetric flask. After dissolving the powder by manually shaking, the closed volumetric flask was left to rest on the laboratory bench for three days. During that time, a

precipitate formed at the bottom of the flask with a strong-yellow supernatant solution. The supernatant was removed and labeled **C1**. A dilution of 1.00 mL of **C1** with aqueous sulfuric acid (1 M) in a 10.00 mL volumetric flask produced a light-yellow solution that was labeled **C2**.

Cerium Removal with $\text{SiO}_2@\text{ZrO}_2$. A 200 mg powdered sample of $\text{SiO}_2@\text{ZrO}_2$ was weighed in a 2-mL Eppendorf tube, and 1.000 mL of aqueous acid solution (either **C1** or **C2**) was added. After closing, the Eppendorf tube was shaken manually for 30 s and stirred mechanically (rotational homogenizer) for 4 h. The colloid was centrifuged (5000 rpm, 5 min), the supernatant removed, and the liquid among solid particles was absorbed with clean paper tissue. The paper tissue was pressed with a metallic spatula on the solid in the Eppendorf tube until the capillary rise in the paper stopped. The solid was dried (60 °C, 15 h).

Thermal Treatment of $\text{SiO}_2@\text{ZrO}_2\text{-Ce}$. After grinding in an agate mortar, a powdered sample (150 mg) was loaded in a Pt sample holder and thermally treated under airflow. The sample was heated at 10 °C.min⁻¹ up to either 1000 °C (**T1**) or 1450 °C (**T2**) and cooled at -10 °C.min⁻¹ down to 150 °C with an instrument for thermal gravimetric analysis and differential thermal analysis (EVO2 Plus Rigaku TG8121). Four different materials were obtained, each by duplicate. The process including cerium removal and immobilization is illustrated in Figure 1.

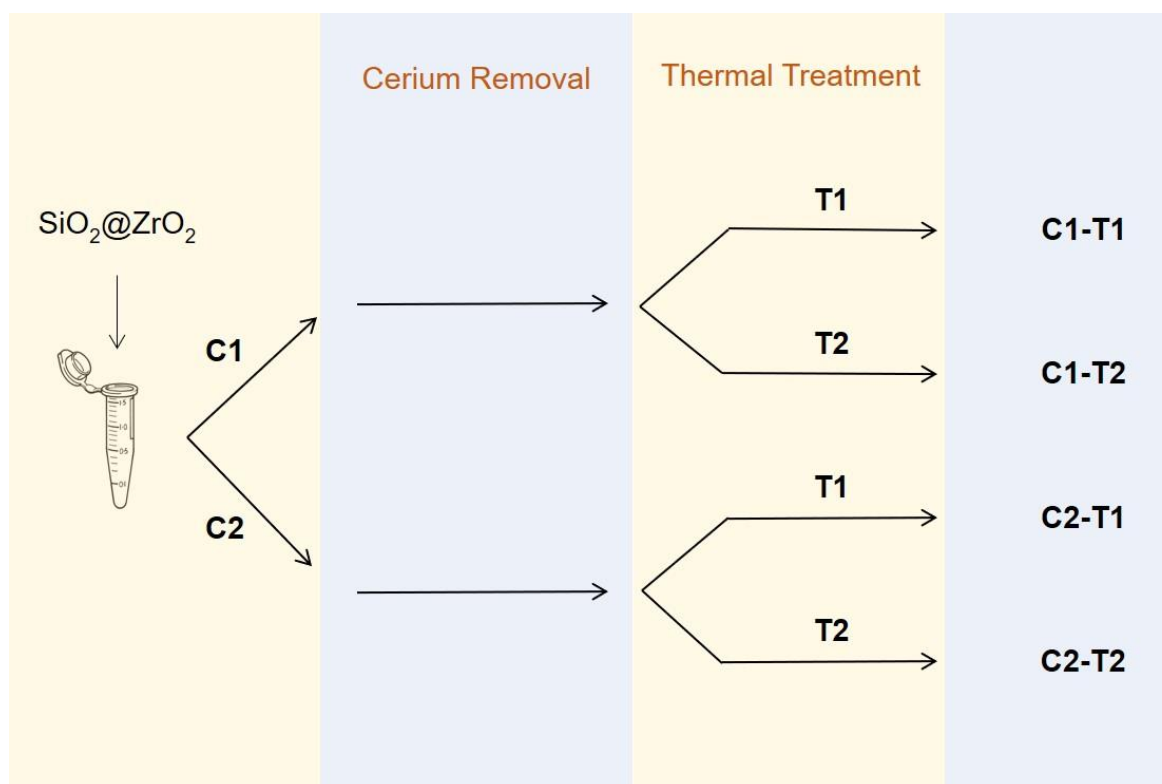


Figure 1. Schematic representation of the process undergone by cs: (a) removal of cerium from solution (**C1** = low cerium concentration and **C2** = high cerium concentration) and (b) heat treatment at two temperatures (**T1** = 1450 ° C and **T2** = 1000 ° C).

Scanning electron microscopy (SEM). Images were obtained using a SEM JEOL JCM-6000 model microscope (30.0 kV). Samples were previously sputtered with gold.

Transmission Electron Microscopy (TEM). Images were obtained using a Hitachi HF-2000 (30 kV). Samples were analyzed either as formed or cut in 30-nm-thick slabs.

Energy-dispersive X-ray spectroscopy (EDX).

X-ray Diffraction (XRD). Diffractograms were obtained with a diffractometer (Cu 1.54060 Å; 40 kV; 40 mA; step 0.2; time/step 50 s) in transmission mode. Reflexes were assigned based on Powder Diffraction Data Base version PDF-2 from International Centre for Diffraction Data (ICDD).

Statistical Analysis. Results were expressed as mean value \pm standard deviation. Analysis of variance (ANOVA) of thermal gravimetric analysis was conducted using InfoStat (version 20/09/2018). A comparison among mean values was made by Fisher's LSD procedure. Statements of statistical significance refer to a probability of type I error of 5% or less ($p \leq 0.05$).

3. Results

3.1 SiO₂@ZrO₂ Synthesis

The synthesis (see above), performed by duplicate, produced well-defined SiO₂@ZrO₂ particles. Mean diameters were 629 ± 27 and 613 ± 29 nm, and the molar ratio was Si/Zr of 5.3 ± 0.3 (EDX) for both samples.

Before performing batch experiments to study Ce removal, we mixed particles from both syntheses to create a starting material. Then, we used this mixture for all batch experiments.

3.2 SiO₂@ZrO₂ Removes Ce

We investigated the ability of SiO₂@ZrO₂ to remove Ce in batch systems. There, Ce solutions had either a **C1** or a **C2** concentration. Then, we characterize the presence of Ce in SiO₂@ZrO₂ with three complementary experiments: (a) visual observation of the solid, (b) elemental analysis (EDX), and (c) TGA.

Visual inspection suggests the presence of Ce in SiO₂@ZrO₂ after the batch experiments. SiO₂@ZrO₂ is a white solid. Ce solutions are yellow with a color whose intensity increases with increasing Ce concentration. Experiments with **C2** solutions produced a light-yellow solid; experiments with **C1** produced a dark-yellow solid.

Elemental analysis (EDX) indicates the presence of S and Ce —besides Si, Zr, and O— in the yellow solid after batch experiments. We observed a significant increase in both the Ce concentration and the S concentration in $\text{SiO}_2@\text{ZrO}_2$ with the increase in the concentration of the batch system solution. The concentration of Ce and S in untreated $\text{SiO}_2@\text{ZrO}_2$ is below the detection limit. On the other hand, the concentration of Ce increased significantly to 0.02 ± 0.01 mol% (light yellow solid) and 0.2 ± 0.1 mol% (dark yellow solid), while the concentration of S increased to 2.6 ± 0.2 mol% and 6 ± 2 mol % S, respectively.

The ATG shows that $\text{SiO}_2@\text{ZrO}_2$ experiences a significant mass loss between 600 and 900 °C the higher the concentration of Ce in solution. The solid untreated in batch systems experiences a loss **Figure 2** of mass of 1%. On the other hand, the mass loss increases significantly to 3 and 7% after treatment in a batch system with solutions whose concentrations were **C2** and **C1**, respectively (ANOVA, $p < 0.0001$) (see Figure 2).

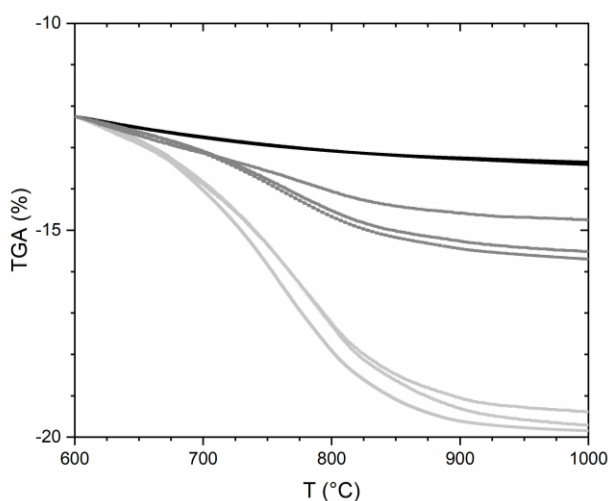


Figure 2. Mass loss between 600 and 900 °C significantly increased from SiO_2 spheres (top, black lines) to SiO_2 exposed to low cerium concentration (middle, dark gray lines), and from the latter to SiO_2 exposed to high cerium concentration (bottom, light gray) (ANOVA & LSD Fisher test, $\alpha = 0.05$). For the sake of comparison, all curves were vertically shifted to make them coincide at $T = 600$ °C.

In short, the experimental evidence supports the ability of dispersed $\text{SiO}_2@\text{ZrO}_2$ particles to remove Ce (and also S) from solution.

3.3 Thermal Treatment Transforms $\text{SiO}_2@\text{ZrO}_2$

To investigate the formation of glass-ceramics, we thermally treated the solids with a TGA-DTA setup (airflow) up to either 1000 or 1450 °C. During heat treatment, we acquired a DTA. After heat treatment, we characterize the solid product with (a) TEM, (b) element mapping with EDX, and (c) XRD.

All DTA results show a similar pattern around 900 °C: a slight endothermic process precedes an intense exothermic process peaking around 900 °C (see, for instance, Figure 4).

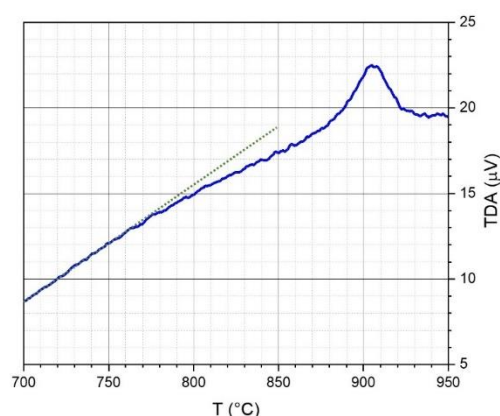


Figure 3. DTA-curve (blue) obtained for $\text{SiO}_2@\text{ZrO}_2$ not exposed to Ce solution. Dotted green line stresses the low endothermic process preceding the clear exothermic process centered around 900 °C.

TEM-images reveal that particles changed their shape after a heat treatment up to 1450 °C, but remained spherical when heated only up to 1000 °C. After experiencing 1450 °C, the resulting particles have more irregular shapes and bigger sizes than the original particles (see Figure 5). Moreover, the resulting particles have a continuous structure (clear in TEM

images) that embeds spheroidal domains (dark in the TEM images). Upon magnification, spheroids seem to have a periodic ordering that suggests the presence of a crystalline structure. After experiencing 1000 °C, particles shrank, and their shells transformed (see Figure 3). Instead of a well-defined shell, thermally treated particles have a continuous phase that embeds nanometric-sized spheroidal domains in a region no deeper than 50 nm from the outer surface.

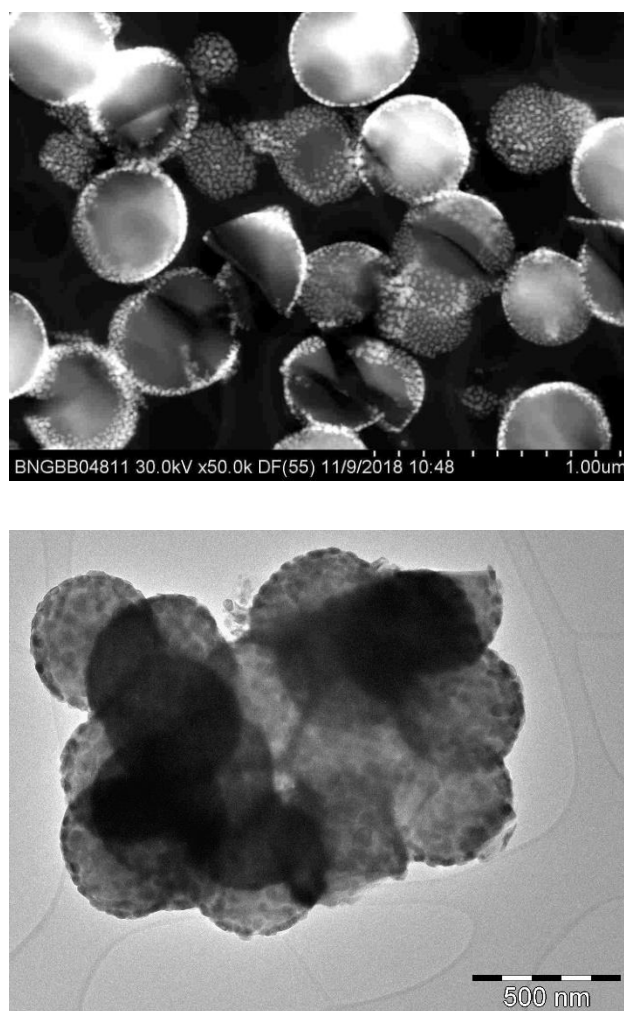


Figure 4. Top: TEM-images of slabs cut from particles heated up to 1000 °C. Spheroidal domains (bright) located near the surface but within spherical. Bottom: TEM-images of uncut samples.

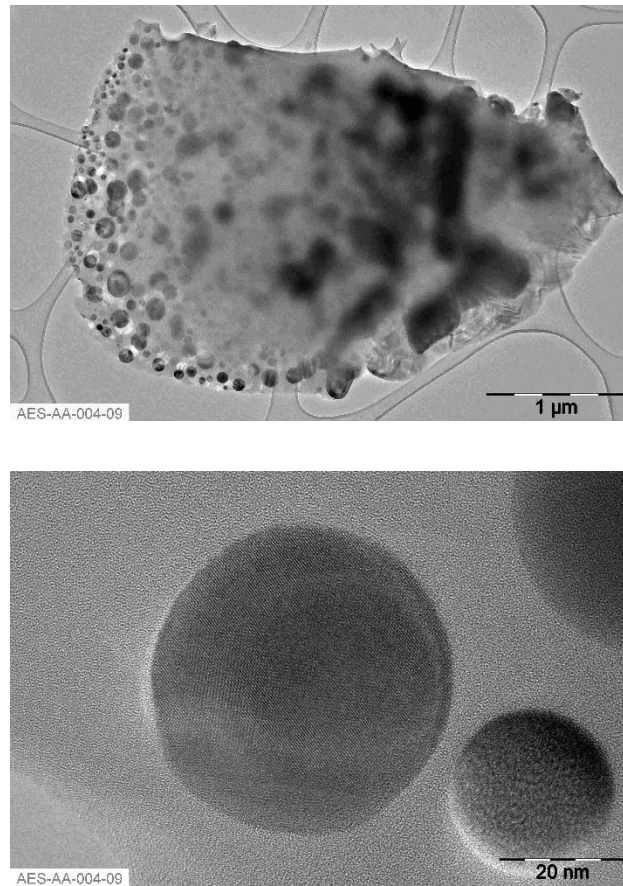


Figure 5. Transmission-electron-microscopy-images from a particle obtained after heating up to 1450 °C. The sized of the particle indicates that this particle formed after sintering many smaller core@shell particles. Spheroidal domains with a darker contrast distribute within a matrix with a lighter contrast. The top-image blurs in the middle because this zone is out of focus.

Element mapping with EDX shows the presence of Ce and Zr in the spheroids and Si in the continuous matrix and Figure 6 the presence of O throughout the material. We can observe this distribution of elements in materials heated up to 1450 °C (Figure 6). However, this distribution of elements is less evident in materials heated up to 1000 °C (see Figure 7).

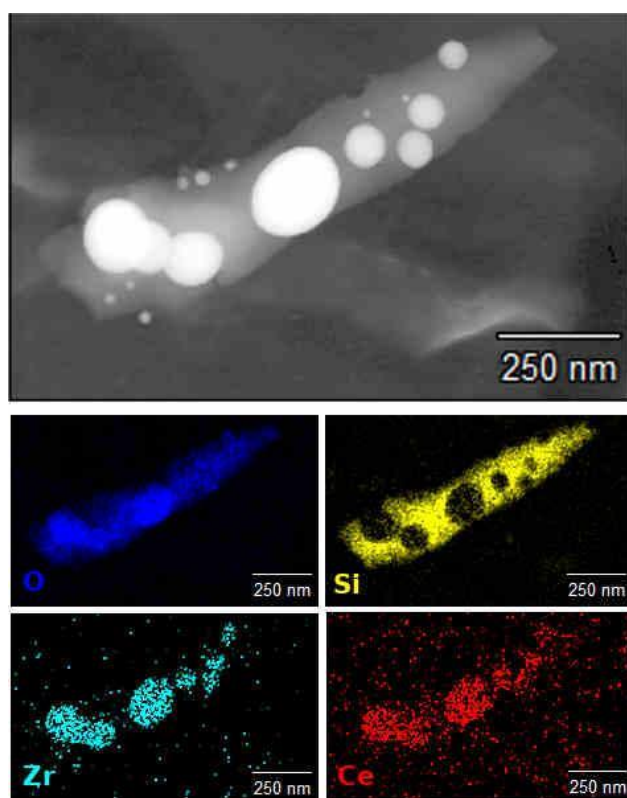


Figure 6. High-resolution Scanning electron microscopic image from a 30 nm thick slab cut from the $\text{SiO}_2@\text{ZrO}_2$ exposed to the solution of Ce and afterward thermally treated up to 1450 °C (top). Images obtained after mapping with Energy-dispersive X-ray spectroscopy the elements oxygen (middle-left), silicon (middle-right), zirconium (bottom, left), and cerium (bottom-right).

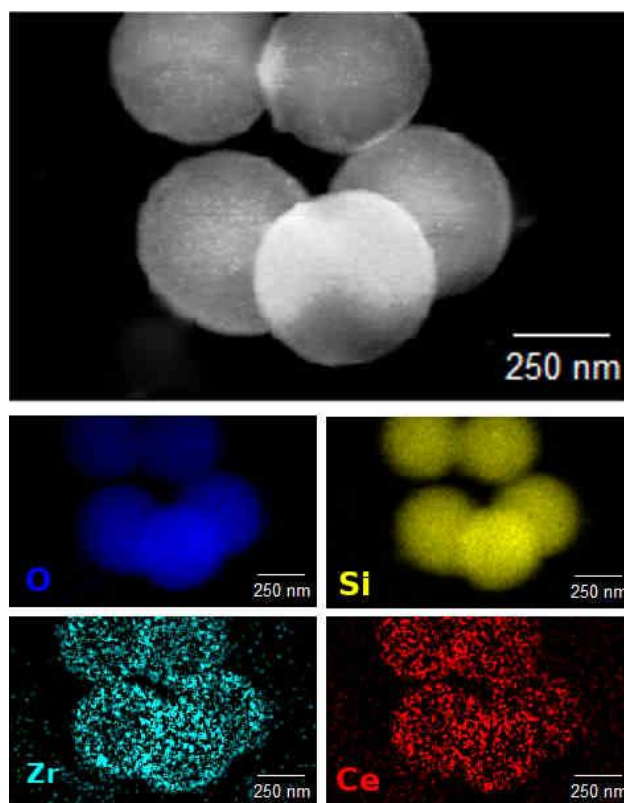


Figure 7. High-resolution Scanning electron microscopic image from $\text{SiO}_2@\text{ZrO}_2$ exposed to the solution of Ce and afterward thermally treated up to 1000 °C (top). Images obtained after mapping with Energy-dispersive X-ray spectroscopy the elements oxygen (middle-left), silicon (middle-right), zirconium (bottom-left), and cerium (bottom-right).

The diffractograms obtained with XRD show the presence of crystals in the heat-treated materials. The presence of Ce seems to influence crystallization. For materials without Ce heated up to 1000 °C, diffractograms have broad reflections assigned to tetragonal ZrO_2 crystals. In contrast, in the presence of Ce, diffractograms with narrow reflections of various crystalline phases (Table 1). On the other hand, the amount of Ce present in $\text{SiO}_2@\text{ZrO}_2$ and the maximum temperature seem to determine which crystalline phases form.

Table 1. Crystalline phases found in the materials were heat-treated at 1000 ° C (column 2) and 1450 ° C (column 3) after they underwent treatment in a sealed system with cerium solutions with concentrations C1 and C2. The bottom row shows the crystalline phases observed in the materials that did not receive a systematic batch treatment to remove cerium as a negative control group.

	1000 °C		1450 °C	
C1	t-ZrO ₂	t-ZrO ₂	t-ZrO ₂	t-ZrO ₂
	m-ZrO ₂	m-ZrO ₂	m-ZrO ₂	m-ZrO ₂
	SiO ₂	SiO ₂	SiO ₂	SiO ₂
	Zr(SiO ₄)	Zr(SiO ₄)		
C2	t-ZrO ₂	t-ZrO ₂	t-ZrO ₂	t-ZrO ₂
			m-ZrO ₂	m-ZrO ₂
	SiO ₂	SiO ₂		
	Zr(SiO ₄)	Zr(SiO ₄)		
(-) ctrl	t-ZrO ₂		t-ZrO ₂	
			m-ZrO ₂	
			SiO ₂	

4. Discussion

4.1 SiO₂@ZrO₂ Recovers Ce from Solution

The experiments carried out in the first part of this work —visual observation, EDX, and ATG— indicate SiO₂@ZrO₂'s ability to recover Ce from aqueous solution. Also, these experiments seem to provide preliminary information on how SiO₂@ZrO₂ removes Ce.

The dispersed colloid removes chemical species with Ce from the solution. After batch experiments, the solid acquires the characteristic yellow color of chemical species with Ce. In addition, Ce and S, the latter coming from sulfate, are found on the surface of the colloid. The removal of Ce from the solution appears to involve a complex process. In a simple adsorption process, we could imagine that a particular type of functional group on the solid surface can anchor the chemical species of Ce. However, Ce forms in sulfuric acid solution various chemical species whose first coordination spheres can include from none to a few sulfate anions. Consequently, a simple mechanism predicts a S/Ce ratio with a value somewhere between 0 and 3 (0 would indicate that none of the chemical species possess sulfate in their sphere of coordination; 3 would indicate that the chemical species of Ce possess on average 3 sulfates for each atom of Ce).

The high S/Ce ratio found in this work —ca. 30 and 130 for $\text{SiO}_2@\text{ZrO}_2$ exposed to **C1** and **C2**, respectively — indicates that $\text{SiO}_2@\text{ZrO}_2$ removes Ce with a complex mechanism. The variation of the S/Ce ratio is incompatible with a simple adsorption mechanism in which one type of functional group on the surface of $\text{SiO}_2@\text{ZrO}_2$ anchor species of Ce. In turn, the increase in S/Ce in $\text{SiO}_2@\text{ZrO}_2$ when the concentration of Ce in solution decreases suggests that $\text{SiO}_2@\text{ZrO}_2$'s surface can directly anchor sulfate anions. Let us remember that at around $\text{pH} = 1$, Ce can form species with both negative and positive charges [17]. It is clear that a mechanistic study that explains how the colloid removes Ce requires more experimental work.

TDA experiments suggest that colloid particles have a material that decomposes chemically and forms volatile species when the temperature exceeds 600 °C. Before treatment in a batch system, the solid loses only 1% of its mass. This loss of mass is compatible with the dehydration of Si-OH and Zr-OH groups that causes the release of H_2O molecules. However, after treatment in a batch system, the solid experiences a significant mass loss:

3% when exposed to **C2** and 7% when exposed to **C1** (see Figure 3). If we consider that $\text{Ce}(\text{SO}_4)_2$ decomposes between 600 and 700 °C [18], we can infer that the mass loss possibly originates from the decomposition of Ce species attached to the surface.

Summing up, $\text{SiO}_2@\text{ZrO}_2$ removes chemical species with Ce presumably following a complex mechanism.

4.2 Thermal Treatment Buries Ce in Glass-Ceramic

The experiments carried out in the second part of this work —TEM, EDX-mapping, XRD, and DTA— indicate the ability of $\text{SiO}_2@\text{ZrO}_2$ to transform upon thermal treatment into a glass-ceramic that buries Ce. This element seems to locate within the ZrO_2 -phase embedded in a continuous SiO_2 -phase.

When the temperature reaches a value approximately equal to half the melting temperature of the solid in degrees Kelvin (Tamman temperature [19]), atoms can diffuse appreciably in the solid. As a result, atoms in a solid may rearrange, and the solid may change its shape.

Upon thermal treatment up to 1450 °C, solid particles experienced an atomic rearrangement and sintered. 1450 °C far exceeds the Tamman temperature of silica (about 700 °C). Above the Tamman temperature, the solid spent ca. 150 min. During that time, atomic diffusion seemed to enable an internal rearrangement of the atoms, which produced a continuous SiO_2 phase containing crystalline ZrO_2 spheroids **Figure 5**Figure 6where Ce atoms locate (see Figure 6 & Figure 7), and seemed to enable the sintering of various particles, which formed larger particles. Similar materials have been obtained upon thermal treatment of Si-Zr-Ce-mixed oxides prepared via a sol-gel synthesis [20].

Upon thermal treatment up to 1000 °C, spherical particles experienced an atomic rearrangement near the surface **Figure 4**and, instead of sintering, they shrunk. 1000 °C exceeds the Tamman temperature of silica (about 700 °C). However, in these experiments,

the solid was 60 min above the Tamman temperature, and the temperature only reached 1000 °C. Under these conditions, atomic diffusion seemed to allow an atomic rearrangement near the surface. The ZrO₂ shell with Ce on its surface transformed into a silica matrix that embedded nanometric spheroids of ZrO₂ containing Ce. In each particle, spheroids situate somewhere within the outer surface and a depth of about 50 nm. Moreover, instead of sintering, spherical particles kept their shape but shrunk.

Besides rearranging atoms and sintering particles, the thermal treatment seemed to enable the conversion of an amorphous oxide —SiO₂@ZrO₂ with Ce— into a glass-ceramic. Upon heating, a glass-ceramic seems to form at about 900 °C. At that temperature, particles undergo an exothermic process centered around 900 °C, preceded by a less intense endothermic process (see Figure 3). This sequence of endo- and exothermic processes indicates the formation of a glass-ceramic material [21]. In addition, the presence of crystals —ZrO₂, SiO₂, and ZrSiO₄— in the thermally treated materials also supports a glass-ceramic formation. Our previous work shows that heating SiO₂@ZrO₂ provokes ZrO₂ crystallization around 900 °C [8]. The absence of cerium oxide crystals and the presence of Ce and Zr within spheroidal domains suggest that Ce substitutes Zr in the crystalline structures.

4.3 Study Limitations

A limitation of this work is using Ce instead of Pu (or other radioactive actinides). However, replacing Pu for Ce considerably simplified the experiments, and surrogating radioactive elements by stable isotopes with similar chemistry is an experimental tactic used in previous studies [20], [22].

Another limitation of this work is the absence of a detailed speciation of Ce in solution, the mechanisms that these chemical species follow to anchor to SiO₂@ZrO₂, and the

determination of optimal removal conditions of Ce. Although these studies would provide valuable knowledge, we can skip them in this first exploratory study.

4.4 Outlook

This study indicates that $\text{SiO}_2@\text{ZrO}_2$ may be an outstanding candidate to test in recovering and immobilizing plutonium and other radioactive actinides. $\text{SiO}_2@\text{ZrO}_2$ recovers actinides such as plutonium, protactinium, americium, and polonium [10]. Moreover, the colloidal size of $\text{SiO}_2@\text{ZrO}_2$ particles may facilitate the formation of glass-ceramics. Because of their colloidal size and nanostructured shell, $\text{SiO}_2@\text{ZrO}_2$ particles have all atomic elements participating in the formation of glass-ceramics next to each other. This proximity may reduce the times and temperatures needed to form a glass-ceramic that stores actinides.

5. Conclusion

This preliminary study suggest that $\text{SiO}_2@\text{ZrO}_2$ has a promising potential in recovering actinides like Pu from water and immobilizing those radioactive elements deep within a glass-ceramic material.

6. Acknowledgments

Pablo M. Arnal would like to thank Prof. Dr. Ferdi Schüth for the invitation to the Max Planck Institute for Coal Research in Germany in September/October 2018; Wolfgang Schmidt and André Pomeroy for helping with software use and sample placement in X-ray diffractometer; and Hans-Josef Bongard and Adrian Schlüter for obtaining high-resolution and transmission electron microscopy images and mapping samples with energy dispersive X-ray spectroscopy. Scientific research commission of the province of Buenos Aires for Ariana's fellowship. National Scientific and Technical Research Council and National Agency for

Scientific and Technical Promotion for financial support: PICT-2014-2583 and PIP-2013/15-0105.

Authors' contributions

Ariana Salvia performed experiments. Pablo M. Arnal performed conceptualization, funding acquisition, experiments, and writing – Original Draft & Review and editing.

7. Bibliography

- [1] W. Runde and M. P. Neu, "The Chemistry of the Actinide and Transactinide Elements," in *The Chemistry of the Actinide and Transactinide Elements*, 4th ed., vol. 6, L. R. Morss, N. M. Edelstein, and J. Fuger, Eds. Springer, 2010.
- [2] R. Dozel, M., Hagemann and A. Chemistry, "COMMISSION ON RADIOCHEMISTRY AND NUCLEAR TECHNIQUES * RADIONUCLIDE MIGRATION IN GROUNDWATERS : REVIEW OF THE BEHAVIOUR OF ACTINIDES Radionuclide migration in groundwaters : Review of the behaviour of actinides (Technical Report)," *Pure and Applied Chemistry*, vol. 65, no. 5, pp. 1081–1102, 1993.
- [3] T. Gäfvert, C. Ellmark, and E. Holm, "Removal of radionuclides at a waterworks," *Journal of Environmental Radioactivity*, vol. 63, no. 2, pp. 105–115, 2002, doi: 10.1016/S0265-931X(02)00020-6.
- [4] K. L. Nash, C. Madic, J. N. Mathur, and J. Lacquement, "Actinide Separation Science and Technology," in *The Chemistry of the Actinide and Transactinide Elements*, 4th ed., vol. 4, L. R. Morss, N. M. Edelstein, and J. Fuger, Eds. Springer, 2010.
- [5] J. M. Haschke and J. L. Stakebake, "Handling, Storage, and Disposition of Plutonium and Uranium," in *The Chemistry of the Actinide and Transactinide Elements of the*

- Actinide and Transactinide Elements*, 4th ed., vol. 5, L. R. Morss, N. M. Edelstein, and J. Fuger, Eds. Springer, 2010.
- [6] B. E. Burakov, M. I. Ojovan, and W. E. Lee, *Crystalline Materials for Actinide Immobilisation*. Imperial College Press, 2011.
 - [7] J. Veliscek-Carolan, "Separation of actinides from spent nuclear fuel: A review," *Journal of Hazardous Materials*, vol. 318, pp. 266–281, 2016, doi: 10.1016/j.jhazmat.2016.07.027.
 - [8] P. M. Arnal, "The synthesis of monodisperse colloidal core@shell spheres and hollow particles," Ruhr-Universität Bochum, Bochum, 2006.
 - [9] P. M. Arnal, C. Weidenthaler, and F. Schüth, "Highly monodisperse zirconia-coated silica spheres and zirconia/ silica hollow spheres with remarkable textural properties," *Chemistry of Materials*, vol. 18, no. 11, pp. 2733–2739, 2006, doi: 10.1021/cm052580a.
 - [10] P. J. Lebed, D. Larivière, I. Maisuls, and P. M. Arnal, "Core@shell and @shell Colloidal Particles Based on a Zirconia Shell Applied to the Extraction of Radioelements," 2014.
 - [11] C. Lopez, X. Deschanel, J. M. Bart, J. M. Boubals, C. Den Auwer, and E. Simoni, "Solubility of actinide surrogates in nuclear glasses," *Journal of Nuclear Materials*, vol. 312, no. 1, pp. 76–80, 2003, doi: 10.1016/s0022-3115(02)01549-0.
 - [12] J. A. Fortner, E. C. Buck, A. J. G. Ellison, and J. K. Bates, "EELS analysis of redox in glasses for plutonium immobilization," *Ultramicroscopy*, vol. 67, no. 1–4, pp. 77–81, 1997, doi: 10.1016/s0304-3991(96)00108-8.
 - [13] H. S. Kim, C. Y. Joung, B. H. Lee, J. Y. Oh, Y. H. Koo, and P. Heimgartner, "Applicability of CeO₂ as a surrogate for PuO₂ in a MOX fuel development," *Journal*

- of *Nuclear Materials*, vol. 378, no. 1, pp. 98–104, Aug. 2008, doi: 10.1016/J.JNUCMAT.2008.05.003.
- [14] J. Diwu, S. Wang, Z. Liao, P. C. Burns, and T. E. Albrecht-Schmitt, “Cerium(IV), Neptunium(IV), and Plutonium(IV) 1,2-Phenylenediphosphonates: Correlations and Differences between Early Transuranium Elements and Their Proposed Surrogates,” *Inorganic Chemistry*, vol. 49, no. 21, pp. 10074–10080, Nov. 2010, doi: 10.1021/ic1015912.
- [15] R. Marsac, F. Réal, N. L. Banik, M. Pédrot, O. Pourret, and V. Vallet, “Aqueous chemistry of Ce(IV): Estimations using actinide analogues,” *Dalton Transactions*, vol. 46, no. 39, pp. 13553–13561, 2017, doi: 10.1039/c7dt02251d.
- [16] K. I. Kuramoto, S. Muraoka, Y. Makino, T. Yanagi, and Y. Ito, “Development of zirconia and alumina based ceramic waste forms for high concentrated TRU elements.” 1995.
- [17] J. Michnyóczy, V. Kiss, and K. Ősz, “A kinetic study of the photooxidation of water by aqueous cerium(IV) in sulfuric acid using a diode array spectrophotometer,” *Journal of Photochemistry and Photobiology A: Chemistry*, vol. 408, 2021, doi: 10.1016/j.jphotochem.2020.113110.
- [18] J. A. Poston, R. V. Siriwardane, E. P. Fisher, and A. L. Miltz, “Thermal decomposition of the rare earth sulfates of cerium(III), cerium(IV), lanthanum(III) and samarium(III),” *Applied Surface Science*, vol. 214, no. 1–4, pp. 83–102, 2003, doi: 10.1016/S0169-4332(03)00358-1.
- [19] F.; Schüth, “General principles for the synthesis and modification of porous materials,” in *Handbook of Porous Solids*, vol. 1, F.; Schüth, S. W.; Kenneth, and J.; Weitkamp, Eds. Weinheim: Wiley-VCH, 2002, pp. 535–666.

- [20] S. V. Ushakov *et al.*, "Synthesis of Ce-Doped Zircon by a Sol-Gel Process," in *Mater. Res. Soc. Symp. Proc.*, 1998, vol. 506, pp. 281–288. doi: 10.1557/PROC-506-281.
- [21] J. Deubener *et al.*, "Updated definition of glass-ceramics," *Journal of Non-Crystalline Solids*, vol. 501, pp. 3–10, Dec. 2018, doi: 10.1016/J.JNONCRY SOL.2018.01.033.
- [22] M. V. Zamoryanskaya and B. E. Burakov, "Feasibility limits in using cerium as a surrogate for plutonium incorporation in zircon, zirconia and pyrochlore," *Materials Research Society Symposium - Proceedings*, vol. 663, pp. 301–306, 2001, doi: 10.1557/proc-663-301.